

Quantum-mechanical features of helicon wave propagation in n -type InSb

R. N. Singh and N. L. Pandey

Applied Physics Section, Institute of Technology, Banaras Hindu University, Varanasi-221005, India

(Received 29 August 1977)

The role of quantum-mechanical oscillatory relaxation time and high-frequency conductivity in the presence of a strong magnetic field has been studied. Accounting for the oscillatory relaxation process and high-frequency conductivity, the dispersion equation for helicon wave propagation has been derived. The dispersion equation thus obtained has been used to construct the refractive-index surfaces. The effect of magnetic field and the helicon wave frequency on the refractive-index surfaces is shown to introduce deformation which offsets the focusing of the propagating helicon waves. The focusing and the interference of the helicon wave along the magnetic-field direction have been discussed in terms of the energy gap between the Fermi energy and the various Landau levels. The analysis of the dispersion equation for real ω and complex k has been carried out to study the role of convective instability in the InSb sample. The relative growth rate of helicon waves propagating through InSb at 4.2°K has been computed for different values of the applied-magnetic-field strength. It is shown that the helicon waves propagating through the sample undergo a typical oscillation. These oscillations can be used as a diagnostic for determining various parameters of the sample.

I. INTRODUCTION

The propagation properties and diagnostic features of helicon waves are well known.¹⁻⁵ The electron gas in thermal equilibrium supporting the helicon wave interacts through the full set of Maxwell's equations and conforms to the general stability theorem propounded by Newcomb.⁶ As a first approximation, it is assumed that the helicon-wave dispersion is free from the effect of orbital quantization of gyrating electrons. However, in the strong-field regime, $\omega_c\tau \gg 1$, the energy levels with large quantum numbers are characterized by electron-density discontinuities and the helicon waves propagating through the electron gas show strong Shubnikov-de Haas type oscillations.⁷⁻⁹ This situation is best visualized by the generalized Landau quasiparticle picture for fermions where scattering of helicon waves is expressed in terms of fluctuation of Landau quasiparticles.¹⁰ With increasing magnetic field the distortion in the Fermi surface increases. The scattering-matrix element is further affected by the discontinuities or electron population corresponding to higher quantum numbers, which cumulatively results into observed oscillations associated with the damping of helicon waves.¹¹⁻¹⁴

It is well established now that the oscillatory contribution to the helicon-wave dispersion originates primarily in the frequency-independent element of the local conductivity tensor and is dominated by the relaxation phenomena governed by the detailed scattering mechanism. The quantum-mechanical expression for the tensorial conductivity which accounts for electron-electron interactions in the self-consistent-field approximation is

highly appropriate for studying helicon-wave dispersion and propagation features.¹⁵⁻¹⁸ In the quantum limit we consider that the electron-electron interaction basically perturbs the density of quantum states which in turn governs the relaxation process in the system. The expression for the phenomenological collision frequency thus derived exhibits an oscillatory behavior and is obviously an inherent source of oscillations in most of the dispersion and propagation features associated with helicon waves. In Sec. II of this paper the quantum theory relevant to helicon-wave propagation has been briefly described. An appropriate dispersion equation has been chosen and its applicability to helicon-wave propagation and damping has been discussed. Utilizing these features of the dispersion equation and the oscillatory behavior of phenomenological collision frequency discussed in Sec. III, we have studied the nature of refractive-index surfaces. In Sec. IV, we have discussed the various features of the helicon wave propagating through n -type InSb. It is further shown that the refractive-index surfaces thus computed give rise to focusing of the helicon wave along the static magnetic field. It is argued that the oscillatory nature of the phenomenological collision frequency and conductivity distorts the refractive-index surfaces in such a way that the helicon waves propagating along the static magnetic field are modulated or bunched. The dispersion equation has been analyzed in Sec. V to study the instability of propagating helicon waves through InSb. An expression for the growth rate of the convective instability has been obtained and the variation of the growth rate with frequency has been shown. This depicts the oscillations which

primarily arise due to the quantum-mechanical phenomenological collision frequency. Their physical significance and their role in possible diagnostics in the study of solid-state plasma in general and InSb in particular have been discussed. With the limited available data for InSb it is shown that the various features of quantum oscillations may depict important features of the band structure, the Fermi surfaces, the contribution of additional relaxation sources, and many other related features.

II. BASIC QUANTUM-MECHANICAL THEORY

The helicon-wave propagation through solid-state plasma under the strong-magnetic-field regime can be best treated in terms of quantum-mechanical perturbation theory. The energy of free electrons in a specimen of thickness d from quantum-mechanical consideration is written as

$$E_{nl} = \hbar\omega_{nl} = (n + \frac{1}{2})\hbar\omega_c + \left(\frac{\hbar^2}{2m_e^*}\right)\left(\frac{\pi l}{d}\right)^2, \quad (1)$$

where ω_c is the cyclotron angular frequency, n and l are the principal and azimuthal quantum numbers. In a solid-state specimen, the electromagnetic field is determined by the set of Maxwell's equations and the relevant boundary conditions. The electric field of the wave produces the necessary perturbations in the vector potential, which gives the required change in the energy of free electrons

$$\begin{aligned} \Delta E &= \hbar\Delta\omega_{l'l} = \hbar(\omega_{n+1, l'} - \omega_{nl}) \\ &= \hbar\left[\omega_c + \frac{\hbar^2}{2m_e^*}\left(\frac{\pi}{d}\right)^2(l'^2 - l^2)\right], \end{aligned} \quad (2)$$

where l' is the perturbed azimuthal quantum number. In a thin slab specimen, the electric-field and current distributions are easily decoupled and the Schrödinger wave equation can be solved. In a rather standard notation the expression for the current density arising from vector-potential perturbations is written as¹⁹

$$J(z, t) = -\frac{e}{m_e^*} \text{Re} \sum_{n, m, l} (\phi_{n, m, l}^* \left(\frac{\hbar}{i}\nabla + \frac{e}{c}A\right) \phi_{n, m, l}), \quad (3)$$

where the vector potential $\vec{A} = \vec{A}_0 + \vec{A}_1(z, t)$; \vec{A}_0 and $\vec{A}_1(z, t)$ correspond to the static magnetic field and the helicon wave, respectively. For linear response, we allow $A_1(z, t) \ll A_0$. The perturbed wave function in the case of helicon-wave propagation through a thin specimen has been given by Turner and Cochran.¹⁷ The total number of occupied electron states is defined as

$$N = \sum_{nml} |\phi_{nml}|^2. \quad (4)$$

Therefore the perturbing potential in a system is effective only when the initial states are occupied and the final states $n' = n \pm 1$ are empty. The relaxation time τ poorly depends on n , l , and B . Running the summation over all terms except $l' = l \pm 1$ the contribution of the potential perturbation to the high-frequency conductivity was obtained by Turner and Cochran as

$$\sigma = \frac{n_e e^2 \tau}{m_e^* [1 + i(\omega \pm \omega_c)\tau]}. \quad (5)$$

Accounting for the lattice contribution to the refractive index and allowing helicon-wave propagation at an angle θ to the static magnetic field, we write the full dispersion equation as

$$\frac{c^2 k^2}{\omega^2} = \epsilon_L + \frac{\omega_p^2}{\omega(\omega_c \cos \theta - \omega + i\nu)}, \quad (6)$$

where $\omega_p^2 = 4\pi n_e e^2 / m_e^*$ is the plasma frequency and $\nu = 1/\tau$ is the phenomenological collision frequency. This equation is similar to the classical equation often used for various properties of helicon-wave propagation. The basic difference arises because of the involved dependence of the quantum-mechanical perturbation on the relaxation process associated with the system.

III. PHENOMENOLOGICAL COLLISION FREQUENCY

InSb has been chosen to investigate the role of quantum oscillations and study its effect on the helicon-wave propagation. The effect of binary collisions to a very great extent is removed by choosing a specimen with very high purity and subjecting it to very low temperatures. Further, InSb has a very small energy gap, high mobility, and a small effective mass which are useful in manifesting the quantum effect when the specimen is subjected to a high magnetic field. In an ordinary specimen with impurities, the relaxation rate which enters the formulation of the conventional conductivity is defined in the Born approximation as

$$\tau^{-1} = \frac{2\pi c_1 N(E_F)}{\hbar}, \quad (7)$$

where c_1 is an energy parameter of the dimension of the energy square and $N(E_F)$ is the density of states. The density of states in a system subjected to a high magnetic field is written as²⁰

$$\begin{aligned} N(E_F) &= \frac{2\sqrt{2}(eB)^{3/2}}{(2\pi)^2 c^{3/2} \hbar^5 / 2\omega_c} \\ &\times \left[(l + \Delta + \frac{1}{2})^{1/2} + \frac{1}{2} \Delta^{-1/2} - (\Delta + \frac{1}{2})^{1/2} \right]. \end{aligned} \quad (8)$$

The Fermi energy in the quantum limit is expressed in terms of a nondimensional equation,

$$E_F/\hbar\omega_c = I + \Delta + \frac{1}{2}. \quad (9)$$

Making appropriate substitutions from Eq. (9) into Eq. (8) and rearranging the resulting equation we write

$$N(E_F) = N_0(E_F) \left[1 + \frac{\frac{1}{2}\Delta^{-1/2} - (\Delta + \frac{1}{2})^{1/2}}{(E_F/\hbar\omega)^{1/2}} \right]. \quad (10)$$

This equation conforms to a perturbed quantum-mechanical density of states often times written as

$$N(E_F) = N_0(E_F) + N_1(E_F), \quad (11)$$

where the equilibrium density of states is defined as

$$N_0(E_F) = \frac{4\pi m_e^*(2m_e^*E_F)^{1/2}}{(2\pi\hbar)^3}.$$

Comparing Eqs. (10) and (11) we obtained the relative perturbation produced in the system,

$$\frac{N_1(E_F)}{N_0(E_F)} = \left(\frac{\hbar\omega_c}{E_F} \right)^{1/2} \left[\frac{1}{2}\Delta^{-1/2} - (\Delta + \frac{1}{2})^{1/2} \right]. \quad (12)$$

From the basic definition of the relaxation rate given in Eq. (7), we obtain the corresponding perturbation in the phenomenological collision frequency for the specimen,

$$\frac{\nu_1}{\nu_0} = \frac{\nu - \nu_0}{\nu_0} = \left(\frac{\hbar\omega_c}{E_F} \right)^{1/2} \left[\frac{1}{2}\Delta^{-1/2} - (\Delta + \frac{1}{2})^{1/2} \right]. \quad (13)$$

It is obvious from this equation that $\nu = \nu_0$ for a critical value of the energy gap between the Fermi level and the Landau level conforming to

$$\frac{1}{2}\Delta^{-1/2} - (\Delta + \frac{1}{2})^{1/2} = 0$$

or

$$\Delta = 0.3.$$

The energy-width parameter Δ oscillates between the limits 0 and 1 and in so doing the effective collision frequency oscillates around the classical value ν_0 . We have chosen the experimental parameters for InSb at 4.2°K as shown in Table I. Using these parameters the perturbation in the phenomenological collision frequencies was computed and

TABLE I. Experimental parameters for InSb at 4.2°K.

Sample no.	Parameters	Chosen values
1	ω_p	4.5×10^{12} rad sec ⁻¹
2	ν_0	9.0×10^9 rad sec ⁻¹
3	E_F	0.5 meV
4	m_e^*	$0.013m_0$

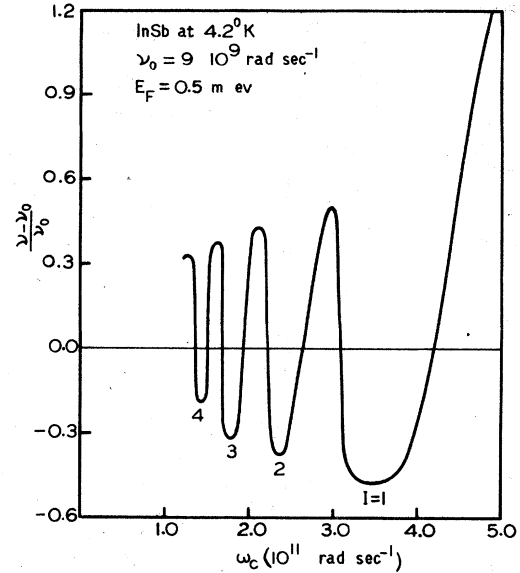


FIG. 1. Variation of the phenomenological collision frequency with applied magnetic field.

its variation with magnetic field is shown in Fig. 1. As the magnetic field changes, the quantum levels accordingly undergo a distributional change which manifest itself in the form of oscillations of various parameters such as the collision frequency, the conductivity, and the conduction current. As the magnetic field in the specimen increases, the magnitude of the oscillations increases and becomes very large for $I=1$, as shown in Fig. 1. With decreasing magnetic field the collision-frequency oscillations decrease in magnitude and are seen to cluster with increasing quantum numbers.

IV. ROLE OF REFRACTIVE-INDEX SURFACES

The dispersion Eq. (6) accounts for the oscillatory nature of the collision frequency. The energy separation between Fermi energy and a particular Landau level has been shown to control the magnitude of the oscillations. Using the method outlined earlier⁴ we have constructed the refractive index surface from the dispersion equation. For a fixed value of I , the refractive surface is seen to show a curious variation with changing $\Omega = \omega/\omega_c$ (Fig. 2). The refractive-index surface depicts a well-defined point of inflexion at $\Omega = 0.20$ whereas the point of inflexion for lower values of Ω loses its significance. The effect of quantum oscillations is shown in Fig. 3. The refractive-index surfaces for a fixed-frequency helicon wave are shown for varying values of energy width between Fermi level and Landau levels. For $\Delta = 0.3$ the collision frequency ν is equal to ν_0 . As Δ increases beyond the critical value the associated resonance peaks

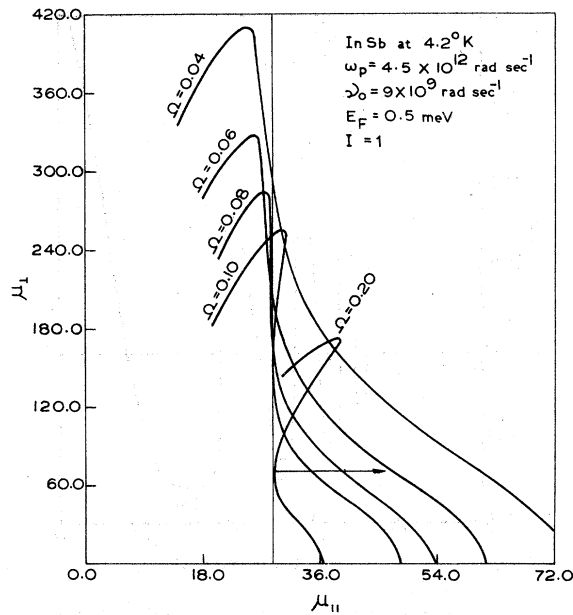


FIG. 2. Frequency dependence of refractive-index surfaces for a helicon wave propagating through InSb.

oscillate as depicted by the dashed lines in Fig. 3. Unlike the picture in Fig. 2, the inflection points in the refractive-index surfaces do not lie along a line and show a significant shift with increasing Δ values. This clearly shows the smearing property of the helicon waves as they propagate in the specimen. The curvatures of the inflection also change with changing values of Δ . Therefore, the propagating helicon waves diffracting differentially from different surfaces interfere

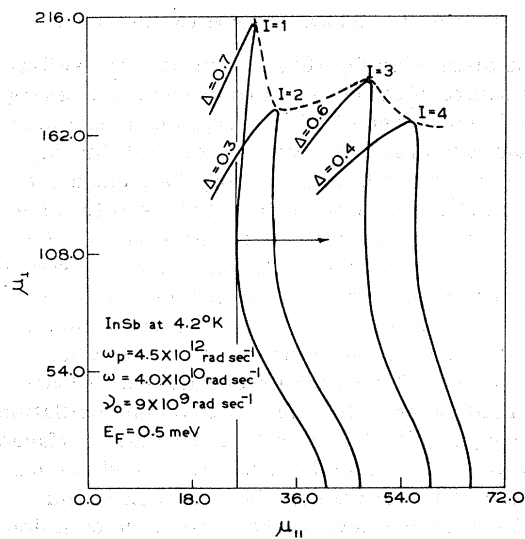


FIG. 3. Quantum oscillations in helicon-wave resonances.

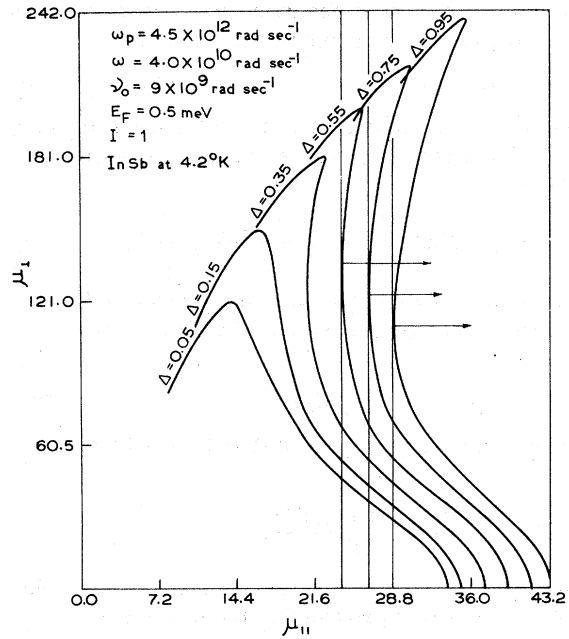


FIG. 4. Effect of band structure on refractive-index surfaces.

so as to produce the oscillatory character of the received helicon waves. A dominant part of this oscillatory behavior arises from the oscillatory nature of the collision frequency which manifests the shape of the refractive-index surfaces and the observed features of the helicon waves propagating through the solid-state specimen.

We have shown that Δ varies between 0 and 1 for each value of I . In Fig. 4 we have shown the variation in the refractive-index surfaces with values of Δ varying from 0.05 to 0.95. The lower values of Δ do not depict the refractive-index surfaces with points of inflection, whereas higher values of Δ show a marked point of inflection which focuses the helicon waves propagating along the static magnetic field in the specimen. For a fixed-frequency helicon wave, $\omega = 4 \times 10^{10}$ rad sec⁻¹, the points of inflection are seen to change with changing values of Δ . For $\Delta = 0.95$ the point of inflection occurs at $\mu_{11} = 28.8$ whereas for $\Delta = 0.75$ the point of inflection shifts to $\mu_{11} = 24$. A ν_0 is taken for the specimen and $\nu = \nu_0$ for $\Delta = 0.3$ has been used. For higher values of Δ the change in collision frequency has been evaluated and accounted for in constructing the surfaces shown in Fig. 4. The refractive-index surfaces seem to be a possible means of manifesting the nature of the helicon wave propagating through the solid-state specimen. The precise knowledge of these surfaces governs the scattering, interference, and focusing of the helicon waves. Diagnostic studies of the helicon-wave

amplitude and phase varying with the magnetic field and temperature can yield very useful parameters for solid-state specimen, namely, carrier density, electron collision frequency, and relaxation parameters. It is well known that the refractive index has a singularity in the absence of collisions. However, in the presence of collisions we find that the resonance feature disappears and the refractive index is limited to a lower value. For a given parallel refractive index there are two perpendicular refractive indices which are characteristic of two modes of helicon-wave propagation. The resonance nose is seen to vary with varying values of Δ . For highest value of $\Delta = 0.95$ the nose appears at ($\mu_{\parallel} = 36$, $\mu_{\perp} = 240$) and is seen to decrease gradually with decreasing values of Δ . The resonance nose is narrow at higher Δ values and becomes broad at lower Δ values.

V. INSTABILITY

The helicon wave propagating with small attenuation through the semiconductor plasma grows either in space or in time. When the amplitude of the propagating-field vectors increases with time, the resulting instability is said to be an absolute instability. The growth of propagating-field vectors in space is known as convective instability. The instabilities of the helicon wave under various conditions have been studied by many workers.²¹⁻²³ The boundary conditions encountered in solid-state plasma often exhibit the onset of absolute instability. Therefore, in this section, we have studied the role of convective instability which arises due to the change in collision frequency in the presence of a static magnetic field. We have analyzed the dispersion Eq. (6) for real ω and complex k . Substituting $k = k_r + ik_i$ and separating the real and imaginary parts, we obtain an expression for the relative growth rate of convective instability,

$$r = \frac{\text{Im}(k)}{k_r} = - \frac{z}{2(1 - \Omega) \left(1 + \frac{\epsilon_L \Omega (1 - \Omega)}{\delta^2} \right)}$$

where $\delta = \omega_p / \omega_c$, $z = \nu / \omega_c$ and $\nu = \nu_0 + \nu_1$ is the per-

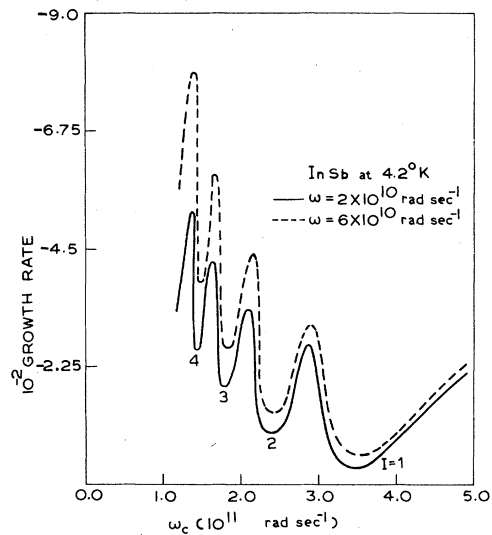


FIG. 5. Variation of relative growth rate with cyclotron frequency.

turbed effective collision frequency. Using the above equation and the parameters for InSb given in Table I, we have computed the relative growth rate of the helicon wave as a function of the applied static magnetic field for fixed values of the helicon frequency. The variation of the relative growth rate with helicon-wave frequency is shown in Fig. 5. The amplitude of the quantum oscillations is seen to be more pronounced for higher values of l . In the presence of a longitudinal magnetic field the spherical Fermi surface is modified, which we have not accounted for in this paper. The oscillations seen in the relative growth rate depicted in Fig. 5 arise chiefly from the quantum-mechanical effect which governs the relaxation processes in the solid-state specimen. A comparison of the nature of the oscillations as depicted theoretically and observed experimentally will reveal interesting diagnostic features.

VI. ACKNOWLEDGMENT

One of us (N.L.P.) is thankful to CSIR, New Delhi, for the award of a Senior Research Fellowship.

¹O. V. Konstantino and V. I. Perel, Zh. Eksp. Teor. Fiz. 38, 161 (1960) [Sov. Phys.-JETP 11, 117 (1969)].

²R. Bowers and M. C. Steele, Proc. IEEE 52, 1105 (1964).

³B. W. Maxfield, Am. J. Phys. 37, 241 (1969).

⁴R. N. Singh and N. P. Pandey, Phys. Rev. B 11, 771 (1975).

⁵N. L. Pandey and R. N. Singh, Phys. Rev. B 14, 719 (1976).

⁶The theorem is proved in an Appendix to I. B. Bernstein, Phys. Rev. 109, 10 (1953).

⁷P. Nozières and D. Pines, Phys. Rev. 109, 1009 (1958).

⁸C. C. Grimes, Plasma Effects in Solids (Dunod, Paris, 1965), p. 87.

⁹J. K. Furdyna, Phys. Rev. Lett. 16, 646 (1966).

¹⁰A. R. Vasconcellos and R. Luzzi, Phys. Rev. B 10, 1773 (1974).

¹¹A. Libchaber and R. Veilex, Phys. Rev. 127, 774 (1962).

- ¹²O. Wolman and A. Ron, Phys. Rev. 148, 548 (1966).
- ¹³A. J. Glick and E. Callen, Phys. Rev. 169, 530 (1968).
- ¹⁴J. K. Furdyna and A. R. Krauss, Phys. Rev. B 2, 3183 (1970).
- ¹⁵N. David Mermin and V. Celli, Phys. Rev. 136, A346 (1964).
- ¹⁶Charles C. Chen and S. Fujita, J. Phys. Chem. Solids 28, 607 (1967).
- ¹⁷R. Turner and J. F. Cochran, Can. J. Phys. 50, 2111 (1972).
- ¹⁸C. S. Ting, S. C. Ying, and J. J. Quinn, Phys. Rev. B 14, 4439 (1976).
- ¹⁹F. Seitz, *Modern Theory of Solids* (McGraw-Hill, New York, 1940).
- ²⁰G. I. Guseva and P. S. Zyryanov, Phys. Status Solidi 25, 775 (1968).
- ²¹G. A. Swartz, J. Appl. Phys. 40, 5343 (1969).
- ²²V. M. Yakovenko, Fizika Tverdogo Tela 14, 299 (1972) [Sov. Phys.-Solid State 14, 249 (1972)].
- ²³N. N. Beletzky, Solid State Commun. 14, 827 (1974).